The influence of plasma density, heating power and plasma shape on type-I ELM energy and particle losses in ASDEX Upgrade

H. Urano, W. Suttrop, L. D. Horton, A. Herrmann, J. C. Fuchs and ASDEX Upgrade Team

Max-Planck-Institut für Plasmaphysik, D-85748, Garching, Germany

1. Introduction

The existing design of ITER requires ELMy H-mode as the reference regime for inductive operation with favourable energy confinement at steady state. However, the energy loss produced by ELM bursts can increase erosion of the divertor targets to the point where component lifetime becomes unacceptably short. A basic observation in several devices is that the ELM energy loss can generally become larger with increasing pedestal stored energy and is reduced with increasing plasma density [1,2]. When the pedestal pressure is limited by type-I ELMs, plasmas with high pedestal temperature T_{ped} or low pedestal density n_{ped} are expected to generate a large ELM energy loss. In a situation of stiff temperature profiles, higher energy confinement is accompanied by higher T_{ped} [3-6]. Mitigating the heat load onto the divertor target simultaneously without deterioration of the energy confinement is a crucial issue in recent ELM studies. In this study, we examine the characteristics of ELM energy and particle losses in type-I ELMy H-modes in ASDEX Upgrade.

2. Experimental data

ELMy H-mode phases in ASDEX Upgrade are selected, which provide maximum variation of upper triangularity δ_u, plasma current I_p, toroidal magnetic field B_t, auxiliary heating power P_{aux} and gas fuelling rate Γ_0. The dataset is restricted to single-null divertor configuration discharges with ion ∇B-drift direction towards X-point. All discharges are fuelled by deuterium gas puffing. All time intervals used in the dataset are selected from stationary phases.

3. ELM energy losses

3.1. Effects of plasma density and shape

Plasma density and shape dependence of ELM energy losses are examined at I_p = 1 MA, B_t = 1.5–2.5 T and the power crossing the separatrix P_{sep} = 4 MW. At fixed P_{sep}, the ELM frequency f_{ELM} and the ELM energy loss ΔW_{ELM} are roughly inversely proportional (see figure 1(a)). While f_{ELM} becomes higher when the pedestal density n_e^{ped} is raised, f_{ELM} decreases with increasing triangularity δ_u at a given n_e^{ped} (see figure 1(b)). From the relation between f_{ELM} and ΔW_{ELM}, one can expect that ΔW_{ELM} increases with increasing triangularity at a given n_e^{ped}.

Figure 2(a) and (b) show the normalised ELM energy loss ($\Delta W_{ELM} / W_{ped}$) as a function of the pedestal electron density normalised to the Greenwald density

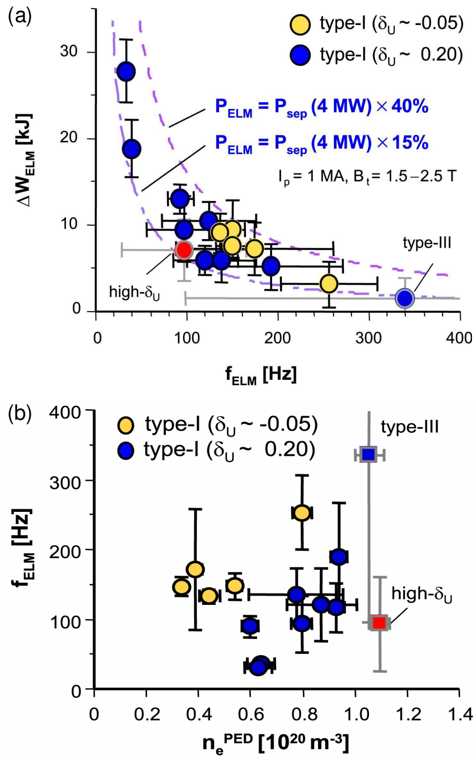

Figure 1. (a) Relation between f_{ELM} and ΔW_{ELM}. (b) Dependence of f_{ELM} on n_e^{ped}.

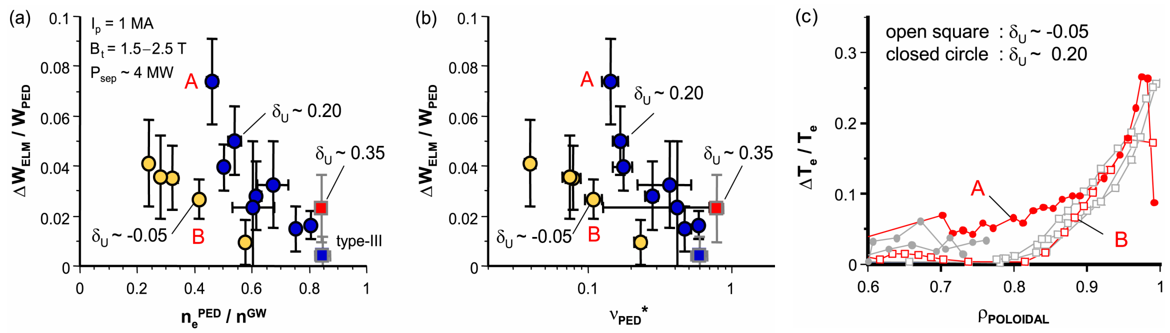

Figure 2. Dependence of $\Delta W_{ELM}/W_{ped}$ on (a) n_e^{ped}/n_{GW} and on (b) ν_{ped}^*. (c) Relative changes to the T_e profiles due to an ELM for the discharges with 0.8 keV < T_e^{ped} < 1.2 keV. Data points A and B discussed in the text are highlighted.

(n_e^{ped}/n_{GW}) and the normalised pedestal collisionality (ν_{ped}^*) for the same discharges as in figures 1, respectively. It can be seen that at fixed I_p, P_{sep} and δ_u the ELM size ($\Delta W_{ELM}/W_{ped}$) decreases with n_e^{ped}/n_{GW} or ν_{ped}^*. However, we also find an explicit difference of $\Delta W_{ELM}/W_{ped}$ between lower and higher δ_u at fixed n_e^{ped}/n_{GW} or ν_{ped}^*. The higher triangularity plasmas obviously produce larger ELM energy losses by a factor of 3-4 than the lower triangularity plasmas at a given n_e^{ped}/n_{GW} or ν_{ped}^*. Note that since ΔW_{ELM} is normalised to W_{ped}, the incease of ΔW_{ELM} with the elevated triangularity is stronger than the increase of W_{ped}. We select two cases for comparison that are marked (A) and (B) in figure 2(a) and (b). These two discharges have different δ_u but similar n_e^{ped}/n_{GW} ~ 0.45 or ν_{ped}^* ~ 0.15. Both cases (A) and (B) are also near T_e^{ped} ~ 1 keV (β_{ped} ~ 0.01). Figure 2(c) plots the relative changes of the T_e profiles due to an ELM measured with the ECE radiometer for the discharges with T_e^{ped} in the range of 0.8-1.2 keV. In figure 2(c), profiles of $\Delta T_e / T_e$ have a peak near the plasma boundary for all discharges with similar relative change. The higher triangularity discharge (A) shows that the ELM perturbation extends radially inward to $\rho_{pol} \le 0.7$, while in the lower triangularity discharge (B) the ELM-affected area extends from the separatrix to ρ_{pol} ~ 0.8, inside which the perturbation rapidly becomes negligibly small. Therefore, the increased ELM energy loss at higher triangularities cannot merely be explained by the increased pedestal pressure but also involve the extended width of the ELM-affected area.

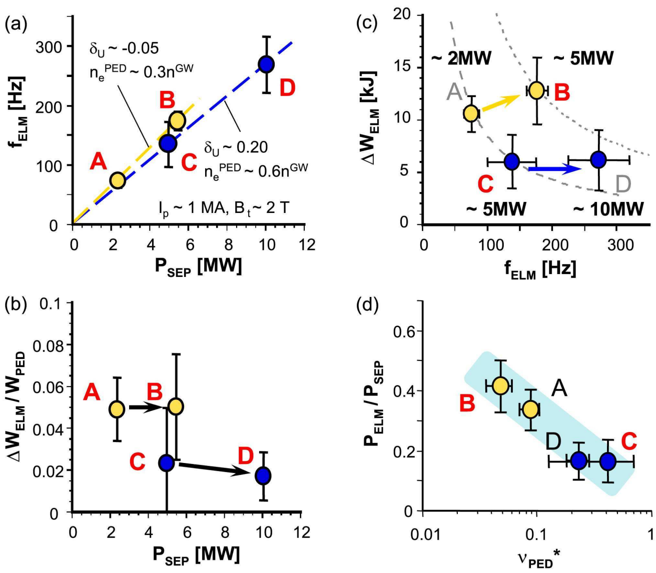

Figure 3. (a) Dependence of f_{ELM} on P_{sep}. (b) Dependence of ΔW_{ELM} / W_{ped} on P_{sep}. (c) Relation between f_{ELM} and ΔW_{ELM}. (d) Dependence of P_{ELM} / P_{sep} on ν_{ped}^*.

3.2. Effects of heating power

The power dependence of ELM energy losses are also investigated for discharges performed at I_p ~ 1 MA and B_t ~ 2 T. In order to analyse the effects of the power crossing the separatrix P_{sep} on ELMs, we select two possible power scans at low (A → B) and high triangularity discharges (C → D) in which P_{sep} is varied over a wide range at a fixed Γ_0. In the discharges (A) and (B) performed at δ_u = -0.05 and Γ_0 ~ 1×10^{21} s^{-1} (n_e^{ped} ~ $0.3n_{GW}$), P_{sep} is varied from 2 to 5 MW, while in the discharges (C) and (D) conducted at δ_u = 0.20 and Γ_0 ~ 3×10^{22} s^{-1} (n_e^{ped} ~ $0.6n_{GW}$), P_{sep} is varied from 5 to 10 MW. Figure 3(a) shows f_{ELM} as a function of P_{sep} for the two power scans (A)-(B) and (C)-(D). We observe that for each case f_{ELM} increases in proportion to P_{sep}. Figure 3(b) shows $\Delta W_{ELM} / W_{ped}$ as a function of P_{sep} for the discharges (A)-(D). The increased power does not change the ELM energy loss for each of the two configurations. From figure 3(a) and (b), one sees that at fixed gas fuelling rate P_{ELM} / P_{sep} remains constant ($P_{ELM} = f_{ELM}\,\Delta W_{ELM} \propto P_{sep}$) because $f_{ELM} \propto P_{sep}$ and $\Delta W_{ELM} \sim const.$ The relation between f_{ELM} and ΔW_{ELM} for the discharges (A)-(D) is plotted in figure 3(c). The data point in each power scan is simply shifted towards larger f_{ELM} by the factor of the increased P_{sep} while ΔW_{ELM} is not changed.

Note that the discharges (B) and (C) are performed at the same P_{sep} of ~ 5 MW with variations of Γ_0 and δ_u. If P_{ELM} was simply proportional to P_{sep}, then f_{ELM} and ΔW_{ELM} would be inversely proportional at fixed P_{sep}. However, figure 3(c) shows that despite of the same P_{sep} the data points (B) and (C) do not follow the expected inverse proportionality. This indicates that there are residual parameters controlling the ELM loss power so that P_{ELM} / P_{sep} is not constant. There is a correlation between ν_{ped}^* and P_{ELM} / P_{sep} as shown in figure 3(d). The fraction of ELM loss power is reduced when ν_{ped}^* is increased since the data points (A)-(D) can be laid on a single trend with the pedestal collisionality. Shown in figure 4 is P_{ELM} / P_{sep} as a function of ν_{ped}^* for the discharges shown in figure 1(a). Regardless of wide ranges of δ_u and Γ_0, we observe the reduction of P_{ELM} / P_{sep} along a single trend with increasing ν_{ped}^*. The pedestal collisionality therefore seems to be playing a key role controlling the ELM loss power P_{ELM}. This finding has implications for the inter-ELM perpendicular transport losses. The dimensionless quantity P_{ELM} / P_{sep} represents the fraction of ELM loss power assigned from the power crossing the separatrix. It follows that the inter-ELM perpendicular transport losses ($1 - P_{ELM} / P_{sep}$) also depends on ν_{ped}^*. Figure 4 amounts to saying that with increasing ν_{ped}^* the inter-ELM perpendicular transport at the plasma edge is enhanced and the ELM transported loss power is reduced.

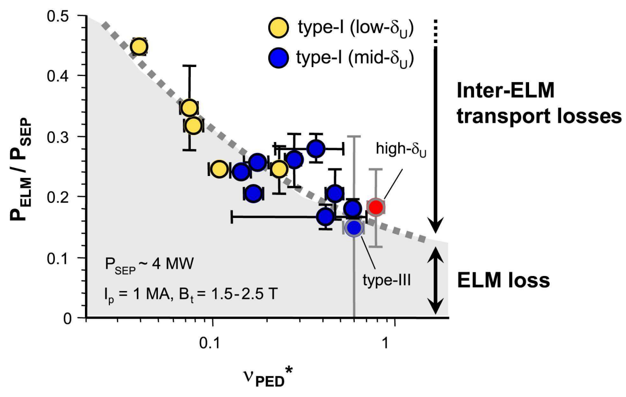

Figure 4. The fraction of ELM loss power (P_{ELM} / P_{sep}) as a function of ν_{ped}^* for the discharges shown in figure 1.

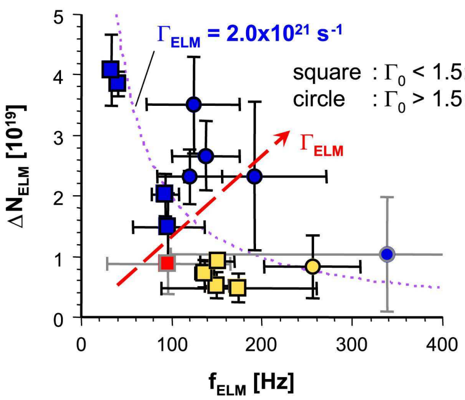

Figure 5. Relation between f_{ELM} and ΔN_{ELM} for the discharges shown in figure 1.

4. ELM particle losses

At a fixed P_{sep} an inverse proportionality between f_{ELM} and ΔW_{ELM} is found with varying Γ_0 in which P_{ELM} remains roughly constant within a finite range (see figure 1(a)). Figure 5 shows the relation between f_{ELM} and ΔN_{ELM} for the same data set in figure 1(a). In figure 5, the data points are classified into two groups of discharges with relatively low Γ_0 (< $1.5\times10^{22}\,s^{-1}$; squares) and high Γ_0 (> $1.5\times10^{22}\,s^{-1}$; circles). It is then seen clearly that the data points with the low Γ_0 exist in the region of low ELM particle flux Γ_{ELM} (= $f_{ELM}\,\Delta N_{ELM}$) bounded by Γ_{ELM} of $2.0\times10^{21}\,s^{-1}$, while those with the high Γ_0 are located inside the region above Γ_{ELM} of 2.0×10^{21} s^{-1}. Thereby, Γ_{ELM} rises with increasing Γ_0. This feature is analogous to the ELM loss power P_{ELM} which rises with increasing P_{sep}. For detailed analysis of the particle balance at the plasma edge, it is desirable to evaluate the particle flux crossing the separatrix Γ_{sep}. Nevertheless, it seems reasonable to use the global parameter Γ_0 as an ordering parameter subsequently. At a fixed Γ_0, f_{ELM} and ΔN_{ELM} in type-I ELMs are roughly inverse proportional to each other in spite of a wide variation of P_{sep}.

5. Discussion and conclusions

The prediction and control of ELM energy loss in type-I ELMs are of significant concern because it is not clear as yet how ELMs of tolerable size can be obtained in a reactor. Integrating the results obtained in this study enables us to identify a scaling for the energy and particle transport of ELMs. Assuming steady state condition, we split energy and particle losses across the separatrix into ELMs and inter-ELM transport phases as follows:

$$P_{sep} = P_{ELM} + P_{transport} \qquad (P_{ELM} = f_{ELM}\,\Delta W_{ELM})$$

$$\Gamma_{sep} = \Gamma_{ELM} + \Gamma_{transport} \approx \Gamma_{ELM} \qquad (\Gamma_{ELM} = f_{ELM}\,\Delta N_{ELM})$$

where $P_{transport}$ and $\Gamma_{transport}$ denote the inter-ELM perpendicular energy and particle transport losses, respectively. In the particle balance, $\Gamma_{transport}$ seems negligibly small. As shown in figures 1(a) and 4, the fraction of ELM loss power P_{ELM} / P_{sep} is not constant but varies in a finite range. With increasing Γ_0, the pedestal collisionality ν_{ped}^* is raised. The increased ν_{ped}^* enhances the inter-ELM perpendicular transport losses and reduces the ELM loss power (see figure 4), i.e. $P_{ELM} / P_{sep} = H(\nu_{ped}^*)$ where the function H seems empirically independent of δ_u. At fixed P_{sep} with a variation of Γ_0 (see figure 5), f_{ELM} increases with increased particle flux across the separatrix. Therefore, the increase of f_{ELM} and the reduction of P_{ELM} with increased ν_{ped}^* force ΔW_{ELM} to decrease with ν_{ped}^* more quickly than f_{ELM} increases.

Taking it into account that f_{ELM} is a function of Γ_{sep} ($f_{ELM} \propto G(\Gamma_{sep})$), we obtain $f_{ELM} = P_{sep} \cdot G(\Gamma_{sep}) \cdot K$, where K is a function of the other parameters such as δ_u. Then, since P_{ELM} ($= f_{ELM}\,\Delta W_{ELM}$) $= \Delta W_{ELM} \cdot P_{sep} \cdot G(\Gamma_{sep}) \cdot K$ and $P_{ELM} / P_{sep} = H(\nu_{ped}^*)$, the ELM energy loss ΔW_{ELM} can be expressed as:

$$\Delta W_{ELM} = \frac{H\left(\nu_{ped}^*\right)}{G\left(\Gamma_{sep}\right)\cdot K}$$

This formula shows why ΔW_{ELM} does not just depend on ν_{ped}^* but also explicitly on plasma shape even if P_{ELM} is a function of pedestal collisionality only. Empirically, $H(\nu_{ped}^*)$ is given to scale approximately as $\nu_{ped}^{*-0.3}$. Knowledge of the functional form of $G(\Gamma_{sep}) \cdot K$, which can be controlling ΔW_{ELM} at a given ν_{ped}^*, is of significant concern and thus will be obtained in a future study.

References

[1] A. Loarte, et al.: Plasma Phys. Control. Fusion **44** (2002) 1815

[2] A. Leonard, et al.: Plasma Phys. Control. Fusion **44** (2002) 945

[3] G. Saibene, et al.: Nucl. Fusion **39** (1999) 1133

[4] G. Janeschtz, et al.: in Proc. of 26th Eur. Conf. on Controlled Fusion and Plasma Physics (Maastricht, 1999) vol 23J (Geneva: EPS) p 1445

[5] J. Stober, et al.: Plasma Phys. Control. Fusion **42** (2000) A211

[6] H. Urano, et al.: Plasma Phys. Control. Fusion **44** (2002) A437